

Cell Reports

Supplemental Information

**Structural and Functional Characterization
of CRM1-Nup214 Interactions Reveals Multiple
FG-Binding Sites Involved in Nuclear Export**

Sarah A. Port, Thomas Monecke, Achim Dickmanns, Christiane Spillner, Romina Hofele, Henning Urlaub, Ralf Ficner, and Ralph H. Kehlenbach

Figure S1

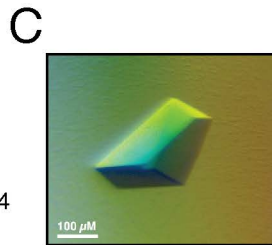
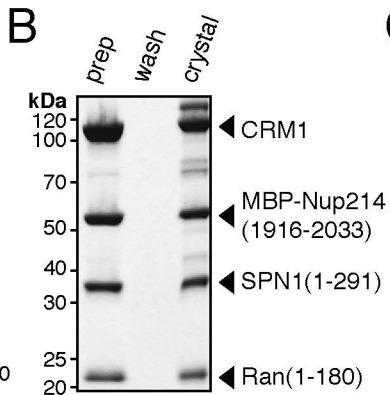
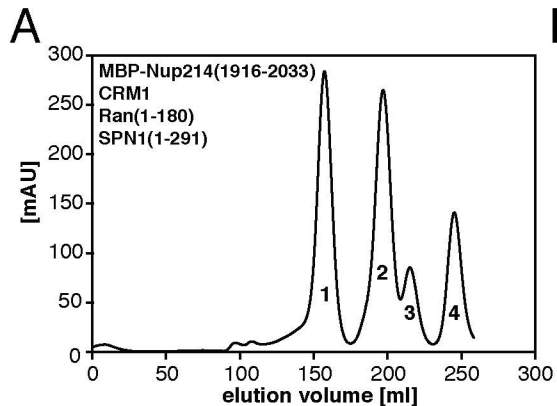
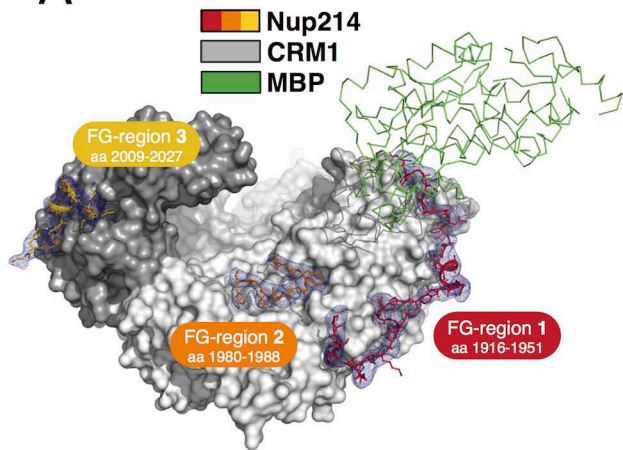
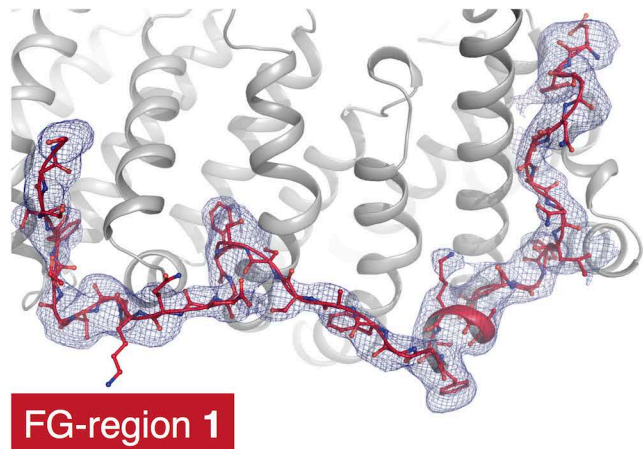


Figure S2

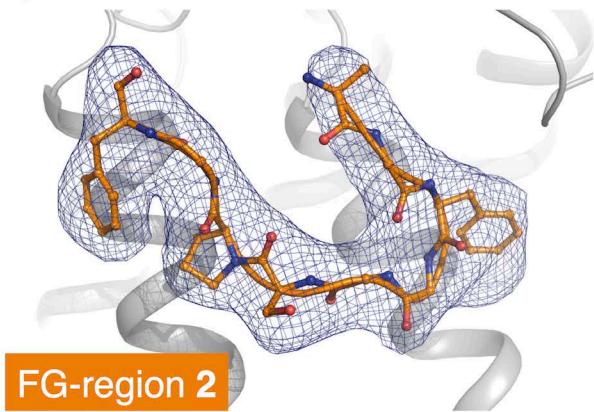
A



B



C



D

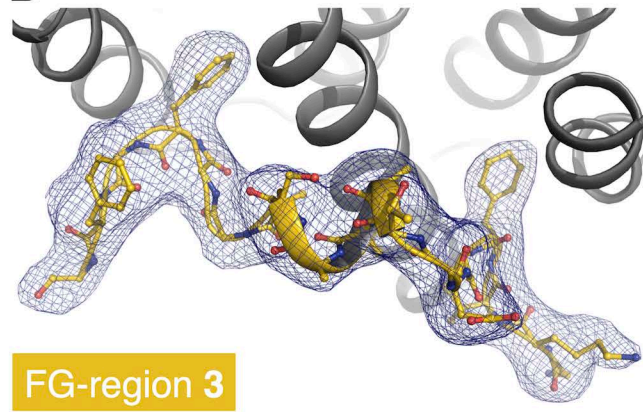


Figure S3

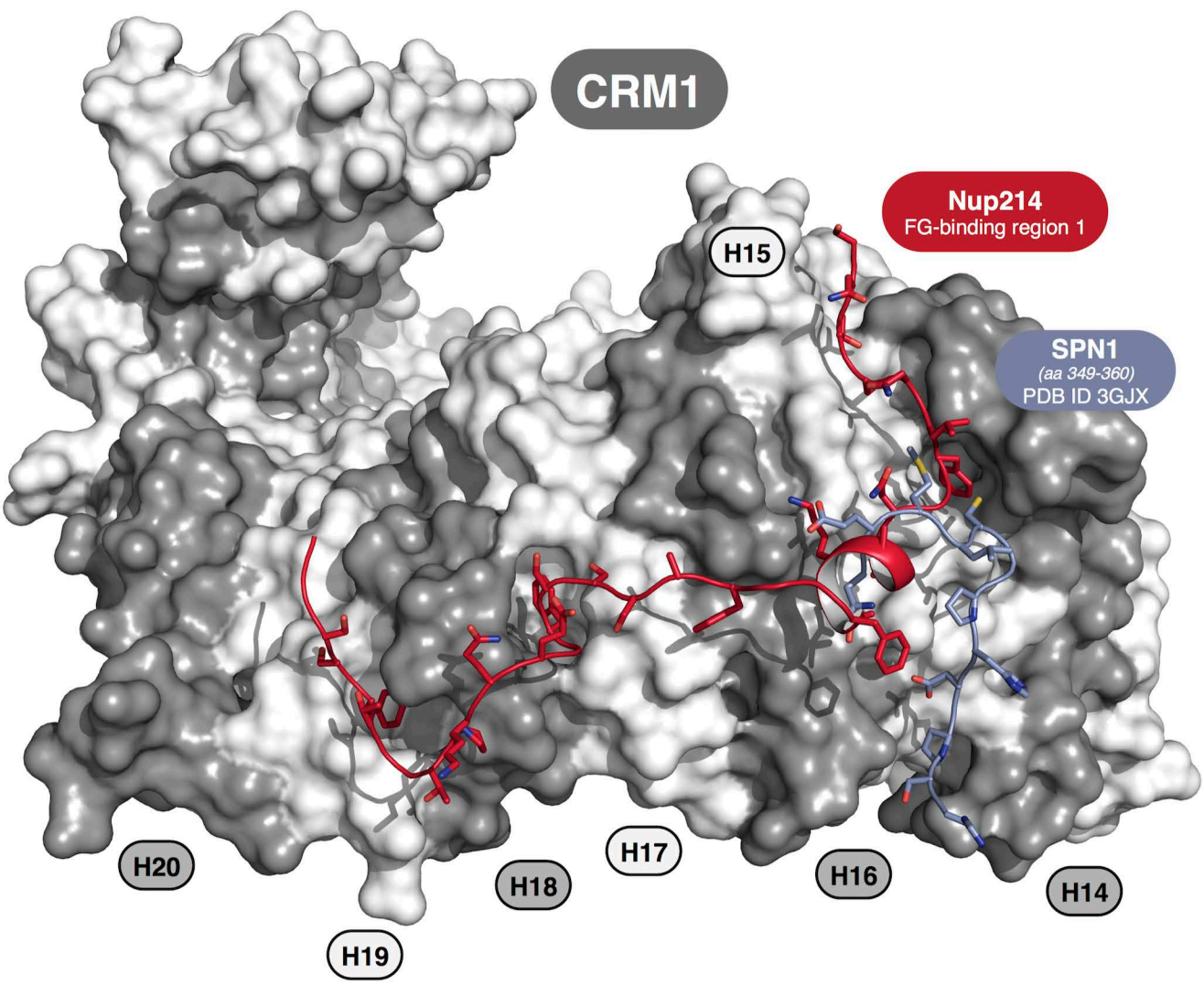
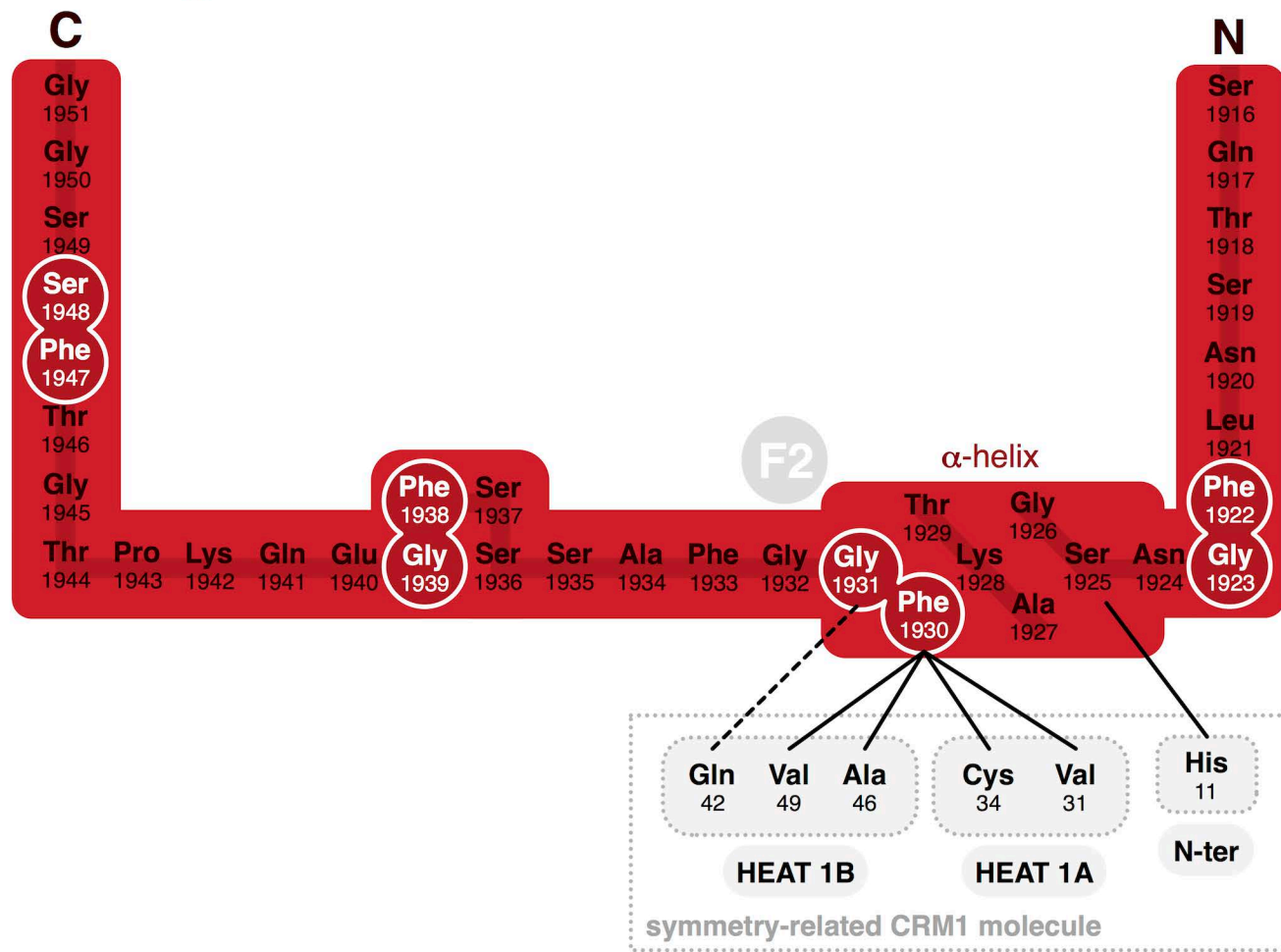
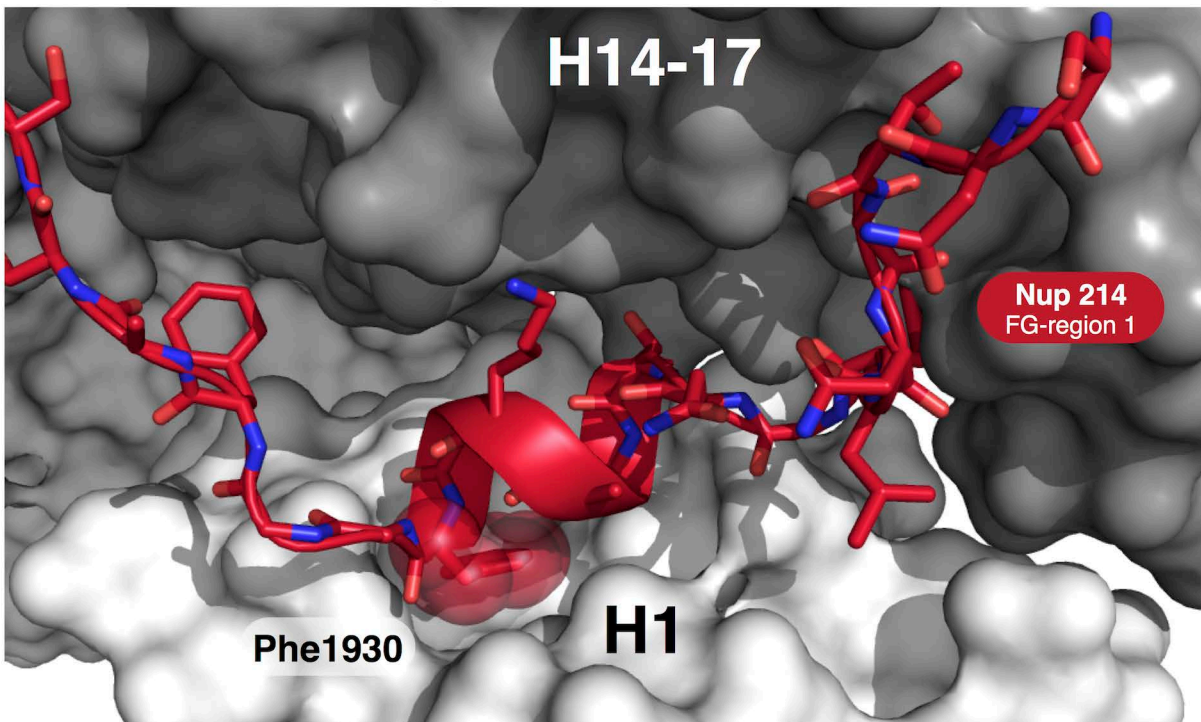


Figure S4

FG-region 1



original CRM1 molecule



symmetry-related CRM1 molecule

Supplemental Figure Legends

Figure S1: Size exclusion chromatography of the Nup214 export complex and analysis of protein crystals; related to Experimental Procedures.

(A) Chromatogram of a Superdex 200 gel filtration run after assembly of CRM1, MBP-Nup214₁₉₁₆₋₂₀₃₃, RanGTP_{1-180, Q69L} and SPN1₁₋₂₉₁. Peak 1 corresponds to the tetrameric complex (compare B, prep), peaks 2, 3 and 4 to excess Nup214, SPN1 and RanGTP, respectively. In the presence of RanGDP instead of RanGTP, no stable complex was formed (data not shown). For SDS-PAGE (B), several crystals (C) were washed (wash) and dissolved (crystal). Proteins were analyzed on a 4-20% gradient gel with subsequent Coomassie staining. Note that all protein components (CRM1, MBP-Nup214, RanGTP and SPN1) are present in the crystals and no significant degradation is observed upon crystallization.

Figure S2: Simulated annealing omit maps for Nup214 FG-regions 1-3 and location of MBP; related to Figure 2.

(A) Representative mFo-DFc simulated annealing electron density omit maps (blue mesh) for individual parts of Nup214 (red, orange or yellow) omitted, as calculated by CNS (Brünger et al., 2007). CRM1 is depicted as surface and gradient colored from grey to white from N- to C-terminus. Nup214 residues are shown as sticks and electron density maps are contoured at a σ -level of 3.0. MBP (green ribbon) was fused to the N-terminus of the Nup214 fragment for crystallization. Detail views on individual FG-regions for Nup214 residues 1916-1951 (FG-region 1) omitted (B), residues 1980-1988 (FG-region 2) omitted (C) and residues 2009-2027 (FG-region 3) omitted (D). CRM1 is depicted in cartoon mode and colored as in A.

Figure S3: Binding sites for the SPN1 C-terminal residues in the ternary export complex and residues of Nup214 FG-repeats (FG-motifs 1-2) on CRM1 partially overlap; related to Figure 2.

CRM1 is shown as surface model and the HEAT repeats (H14-H20) are colored alternating in grey and white. Nup214 residues 1916-1951 bound to the FG-binding patch 1 of CRM1 are depicted in red, while the C-terminal residues of SPN1 bound to the same CRM1 region from the ternary export complex (PDBid 3gix) are colored in blue. Note that the binding sites for both molecules partially overlap on CRM1.

Figure S4: FG-motif 2 interacts with an FG-binding pocket at the N-terminus of a symmetry-related CRM1 molecule; related to Figures 2, 3.

(A) Schematic representation of the interaction between Nup214 in red (1916-1951) and CRM1. The original CRM1 molecule is shown in grey, while the symmetry-related CRM1 molecule contributing the FG-binding pocket for FG-motif 2 (F2) is depicted in white. Polar interactions are represented as dashed lines ($\leq 3.5 \text{ \AA}$) while hydrophobic and van-der-Waals interactions are depicted as solid lines ($\leq 4 \text{ \AA}$). N- and C-termini as well as α -helical regions are labeled. FG-motifs are encircled in white and highlighted. (B) Structural representation showing binding of FG-motif 2 (red) to the symmetry-related CRM1 molecule (white surface). Phenylalanine 1930 of the FG-repeat is illustrated by transparent spheres and labeled.

Figure S5: Protein-protein cross-linking within the trimeric export complex with bound Nup214; related to Figure 3.

(A) MSMS analyses of cross-linked peptides derived from Nup214 and SPN1 (Nup214 K1928 – SPN1 K223) and CRM1 (Nup214 K2010 – CRM1 K22). See also Supplementary

Tables S1 and S2. The sequences of the cross-linked peptides are shown with their respective b- and y-type fragment ions in the spectra. (B) Examples of protein-protein cross-links visualized in the 3D structure of the protein complex.

Figure S6: CRM1 (D824K/W880A) double FG-binding pocket mutant; related to Figure 5.

Pull-downs. (A) 50 pmol GST-Nup214₁₉₆₈₋₂₀₃₃ was immobilized on beads and incubated with 50 pmol of wild type CRM1 or the CRM1 (W880A) mutant and NES peptide in the absence or presence of 150 pmol RanGTP_{Q69L}. Bound proteins were analyzed by SDS-PAGE, followed by Coomassie-staining. (B) 25 pmol of the respective CRM1 mutants were incubated with phenylsepharose in the absence or presence of 75 pmol RanGTP and 2.5 μ M NES peptide. Bound proteins were analyzed by SDS-PAGE, followed by Coomassie-staining.

Table S1: X-ray data collection, refinement and validation statistics for the Nup214 export complex; related to Figure 2

Data collection	
Space group	$C222_1$
Number of complexes in a. u.	1
Wavelength, Å	0.9184
Cell dimensions	
<i>a</i> , <i>b</i> , <i>c</i> ; Å	112.33, 248.97, 210.57
α , β , γ ; °	90.0, 90.0, 90.0
Resolution, Å	48.49-2.85 (2.95-2.85)*
R_{merge}	0.055 (0.571)
R_{meas}	0.062 (0.644)
$CC_{1/2}$	99.9 (87.3)
$I/\sigma(I)$	15.52 (2.01)
Completeness, %	98.2 (91.4)
Multiplicity	4.6 (4.1)
Refinement	
Resolution, Å	30.00-2.85
No. reflections	67922
R_{work}	0.205
R_{free}	0.249
No. atoms	14991
<i>B</i> -factor, Å ²	125.0
r.m.s.d.	
Bond lengths, Å	0.006
Bond angles, °	0.925

* Values in parentheses indicate the specific values in the particular highest resolution shell.

Table S2: intraprotein cross-links; related to Figure 3

Protein	Peptide 1	Peptide 2	Residue 1	Residue 2	Distance 3GJX	Distance
SPN1	RLAEDDWTGMESEENKK	DDEEMDIDTVKKLPK	80	93	ND	ND
SPN1	QTHYSPGSTPLVGLRPYMVSDVLGVAVPAGPLTTKP	KSQK	298	314	ND	ND
SPN1	DYAGHQQLQIMEHK					
SPN1	NSTAKDYTILDCIYNEVNQTYVLDVMCWR	FYWMHSKLPEEEGLGEK	167	211	17.5	18.1
SPN1	LTHKASENGHYELEHLSTPK	TKLNPFFK	327	223	ND	ND
SPN1	ASENGHYELEHLSTPKLK	TKLNPFFK	343	223	ND	ND
SPN1	ASENGHYELEHLSTPKLK	LLELQKSK	343	52	ND	ND
SPN1	ASENGHYELEHLSTPKLK	LSQYKSK	343	32	ND	ND
SPN1	SKYSSLEQSER	LLELQKSK	34	52	29.0	30.6
SPN1	LSQYKSK	EKLTHK	32	323	ND	ND
SPN1	GSTSAYTKSGYCVNR	LSQYKSK	144	32	ND	ND
SPN1	LLELQKSK	EKLTHK	52	323	ND	ND
SPN1	GSTSAYTKSGYCVNR	SKYSSLEQSER	144	34	24.6	23.5
SPN1	LSQYKSK	KSQK	32	314	ND	ND
SPN1	LSQYKSK	KLPK	32	93	ND	ND
SPN1	GSTSAYTKSGYCVNR	KSQK	144	314	ND	ND
SPN1	LLELQKSK	KSQK	52	314	ND	ND
SPN1	LLELQKSK	KLPK	52	93	14.4	14.7
SPN1	TKLNPFFK	KSQK	223	314	ND	ND
CRM1	LHNQVNGTEWSWKNLNTLCWAIGSISGAMHEEDEK	FLVTVIKDLLGLCEQKR	492	522	20.7	20.5
CRM1	ACKAVGHFPFVIQLGR	ETLKLISGWVSR	700	757	10.0	10.2
CRM1	QEWPKHWPTFISDIVGASR	LLSEEVDFSSGQITQVKSK	144	190	12.1	11.8
CRM1	ACKAVGHFPFVIQLGR	QLGSILKTNVR	700	693	10.7	10.7
CRM1	ACKAVGHFPFVIQLGR	EFMKDTSINLYK	700	446	18.5	17.6
CRM1	VDTILEFSQNMNTKYGLQILENVIK	TSSDPTCVEKEK	76	122	11.1	12.1
CRM1	MAQEVLTHLKEHPDAWTR	YYGLQILENVIKTR	54	88	16.4	13.0
CRM1	NLNTLCWAIGSISGAMHEEDEKR	AHWKFLK	514	560	14.4	14.6
CRM1	QEWPKHWPTFISDIVGASR	WKILPR	144	92	12.6	12.9
CRM1	QLLDFSQKLDINLLDNVNVNCLYHGEGAQQR	MPAIMTMLADHAAR	22	1	ND	ND
CRM1	ACKAVGHFPFVIQLGR	IAQKCR	700	594	15.4	15.5
CRM1	EFMKDTSINLYK	IAQKCR	446	594	19.5	19.1
CRM1	ETLKLISGWVSR	QLGSILKTNVR	757	693	9.0	9.0
CRM1	FLVTVIKDLLGLCEQK	GKDNK	522	534	19.4	19.4
CRM1	NVDILKDPETVK	QLGSILKTNVR	680	693	18.7	19.2
CRM1	LLSEEVDFSSGQITQVKSK	WKILPR	190	92	14.1	14.8
CRM1	YYGLQILENVIKTR	WKILPR	88	92	8.9	9.3
CRM1	QADEEKHKR	SKHLK	1049	192	24.3	ND
CRM1	FLVTVIKDLLGLCEQK	AHWKFLK	522	560	15.6	15.8
CRM1	ETLKLISGWVSR	TVKR	757	752	8.7	8.7
CRM1	QADEEKHKR	IAQKCR	1049	594	53.2	ND
CRM1	DTDSINLYKNMR	IAQKCR	455	594	20.2	20.0
CRM1	DLLGLCEQKR	GKDNK	531	534	8.8	8.9
RAN	NLQYYDISAKSNYNFEKPFLWLAR	VCENIPIVLCGNKVDIKDR	152	127	12.7	12.9
RAN	NLQYYDISAKSNYNFEKPFLWLAR	HLTGEFEKK	152	37	8.8	9.2
RAN	VCENIPIVLCGNKVDIKDR	KVKAK	127	132	11.6	11.4
RAN	KYVATLGVEVHPLVFHTNR	TTFVKR	38	28	12.1	11.9
RAN	VTYKNVPNWHR	AKSIVFHR	99	134	14.1	14.1
RAN	VCENIPIVLCGNKVDIK	DRKVK	123	130	10.6	10.7
RAN	VTYKNVPNWHR	KVKAK	99	132	12.8	12.6
RAN	VTYKNVPNWHR	KNLQYYDISAK	142	99	14.8	14.9
RAN	HLTGEFEKK	TTFVKR	37	28	11.1	11.3

Table S3: interprotein cross-links; related to Figure 3

Protein 1	Protein 2	Peptide 1	Peptide 2	Residue 1	Residue 2	Distance
SPN1	CRM1	QLYLPMLFKVR	LSQYKSK	32	415	ND
RAN	CRM1	NLQYYDISAKSNYNFEKPFLLWLR	ETLKLISGWVSR	152	757	20.3
RAN	CRM1	VCENIPVLCGNKVDIKDR	ACKAVGHFVLIQLGR	127	700	17.7
RAN	CRM1	VCENIPVLCGNKVDIKDR	ETLKLISGWVSR	127	757	16.8
RAN	CRM1	VTYKNVPNWHR	QADEEKHKR	99	1049	ND
SPN1	CRM1	LAEDDWTGMESEEEENKKDDEEMDIDTVK	DLLGLCEQKRGK	81	531	ND
SPN1	CRM1	TKLNPFKFGVGLK	NVDILKDPETVK	223	680	10.5
SPN1	RAN	LPEEEGLGEKTKLNPFK	SNYNFEKPFLLWLR	221	159	48.4
CRM1	RAN	LHNQVNGTEWSWKNLNTLCWAIGSISGAMHEEDEKR	SNYNFEKPFLLWLR	492	159	21.3
CRM1	RAN	LFVTGLFSLNQDIPAFKEHLRDFLVQIK	VTYKNVPNWHR	1012	99	16.0
CRM1	SPN1	YMLLPNQVWDSIIQQATKNVDILKDPETVK	TKLNPFK	674	223	17.2
CRM1	RAN	LAYSNGKDEQNFQNLSLFLCTFLKEHDQLIEK	AKSIVFHR	331	134	16.5
CRM1	RAN	RETLKLISGWVSR	HLTGEFEKK	757	37	20.6
CRM1	RAN	CLSENISAAIQANGEMVTQPLIR	HLTGEFEKK	741	37	15.1
CRM1	SPN1	NVDILKDPETVKQLGSILK	TKLNPFK	686	223	14.9
CRM1	SPN1	LHNQVNGTEWSWKNLNTLCWAIGSISGAMHEEDEKR	KLPK	492	93	29.1
CRM1	RAN	MAKPEEVLVVENDQGEVVR	SNYNFEKPFLLWLR	426	159	18.2
CRM1	SPN1	FLVTVIKDLLGLCEQKR	LSQYKSK	522	32	ND
CRM1	SPN1	FLVTVIKDLLGLCEQKR	SKYSSLEQSER	522	34	ND
CRM1	SPN1	AHWKFLK	LSQYKSK	560	32	ND
CRM1	SPN1	CLSENISAAIQANGEMVTQPLIR	TKLNPFK	741	223	20.9
CRM1	SPN1	FLKTVVNK	LSQYKSK	563	32	ND
CRM1	SPN1	GKDNK	KLPK	534	93	14.7
NUP	SPN1	QTVDAALAAAQTNAAAEFNNTSNLFGNSGAKTFGGFA SSSFGEQKPTGTFSSGGGSVASQGFSSPNK	TKLNPFK	1928	223	31.8
NUP	CRM1	TGGFGAAPVFGSPPTFGGSPGFGGVPAFGSAPFTSP LGSTGGKVFGEGTAAASAGGFGGSSSNTTHHHHHH	QLLDFSQKLDINLLDNVVNCLYHGEGAQQR	2010	22	14.2
SPN1	CRM1	DLLGLCEQKR	KLPK	93	531	20.5

Table S4: Plasmids generated in this study; related to Experimental Procedures

Plasmid	Cloning
pQE60-CRM1 (A156F)-His	mutagenesis on pQE60-CRM1-His (5'-ctttatcagtgatattgttgaTTTagtaggaccagcgaaagtctc-3'/ 5'-gagactttcgtggtcctactAAAccaacaatatcactgataaaaag-3')
pQE60-CRM1 (L679R)-His	mutagenesis on pQE60-CRM1-His (5'-caaccaaaaatgtggataCGTaaagatcctgaacagctcaagcag-3'/ 5'-ctgcttgactgttcaggatcttACGtatatccacattttggtg-3')
pQE60-CRM1 (D824K)-His	mutagenesis on pQE60-CRM1-His (5'-ctgaaatcctcaaatattAAAgctgttttgaatgcacattg-3'/ 5'-caatgtgcattcaaaaacagcTTTaaatattgaggtattcag-3')
pQE60-CRM1 (Y918W)-His	mutagenesis on pQE60-CRM1-His (5'-ctcagagttttatcaaaactGGttttgtgatattccagcata-3'/ 5'-tatgctggagaatatcacaaaCCAagtttgataaaaactctgag-3')
pQE60-CRM1 (W880A)-His	mutagenesis on pQE60-CRM1-His (5'-ctgttttggattccatcattGCGgcttcaacatactatgag-3'/ 5'-ctcatagtatgtttgaaagcCGCaatgatggaatcctcaaaaag-3')
pQE60-CRM1 (S928K)-His	mutagenesis on pQE60-CRM1-His (5'-gatattcctcagcatatcttAAGgtgtgacagacacttcac-3'/ 5'-gtgaagtgtctgcacaacCTTaaagatgtctggagaatc-3')
pQE60-CRM1 (D824K/W880A)-His	mutagenesis on pQE60-CRM1 (D824K)-His (5'-ctgttttggattccatcattGCGgcttcaacatactatgag-3'/ 5'-ctcatagtatgtttgaaagcCGCaatgatggaatcctcaaaaag-3')
pQE60-CRM1 (A156F/D824K/W880A)-His	mutagenesis on pQE60-CRM1 (D824K/W880A)-His (5'-ctttatcagtgatattgttgaTTTagtaggaccagcgaaagtctc-3'/ 5'-gagactttcgtggtcctactAAAccaacaatatcactgataaaaag-3')
pGEX-Nup214(1859-2090)	PCR Nup214 (5'-tttGAATTCggaatagctttggccagcaatcctcct-3'/ 5'-tttGTCGACTcagcttcgcccaccacaaaac-3'), cloned into pGEX-6P1 (EcoRI, Sall)
pGEX-Nup214(1930-2021)	PCR Nup214 (5'-tttGAATTCtttgggtgattgccagctcgtcg-3'/ 5'-tttGTCGACTtatgcctgagcagctcagctcagtg-3'), cloned into pGEX-6P1 (EcoRI, Sall)
pmRFP-Nup214(1859-2090)-cNLS	PCR Nup214 (5'-tttGAATTCggaatagctttggccagca-3'/ 5'-tttGTCGACTcagcttcgcccaccacaaaac-3'), cloned into pmRFP-cNLS (Roloff et al., 2013) (EcoRI, Sall)
pmRFP-Nup214(1859-2090)X1/X2/X3-cNLS	synthesized fragments cloned into pmRFP-cNLS (Roloff et al., 2013) (EcoRI, Sall)
pET28a-His-Nup214(1916-2033)X1/X3-His	PCR on pmRFP-Nup214(1859-2090)X1/X3-cNLS plasmids (5'-tttCATATGtcaataaccttaacctatctggaacag-3'/ 5'-tttCTCGAGTgtggtgtgctgctctcc-3'), cloned into pET28a (NdeI, XhoI)
pET28a-His-Nup214(1916-2033)X2-His	PCR on pmRFP-Nup214(1859-2090)X2-cNLS plasmid (5'-tttCATATGtcaataaccttaacctatttggaaacag-3'/ 5'-tttCTCGAGTgtggtgtgctgctctcc-3'), cloned into pET28a (NdeI, XhoI)
pMal-linkerAAA	PCR on pMal-c2 (5'-tttAGATCTgctgccgaaccgcccacaaaacctgg-3'/ 5'-aatGAATTCgcccgcgcatagctcgcgctgccagggtgcatcgacagctc-3'), cloned into pMal-c2 (BglII, EcoRI)
pMal-linkerAAA-Nup214(1916-2033)X1/X3-His	PCR on pmRFP-Nup214(1859-2090)X1/X3-cNLS plasmids (5'-tttGAATTCtcaataaccttaacctatctggaacag-3'/ 5'-tttGTCGACTtagtgatggtgatggtgatggtgtgctgctctcc-3'), cloned into pMal-linkerAAA (EcoRI/Sall)
pMal-linkerAAA-Nup214(1916-2033)X2-His	PCR on pmRFP-Nup214(1859-2090)X2-cNLS plasmid (5'-tttGAATTCtcaataaccttaacctatttggaa-3'/5'-tttGTCGACTtagtgatggtgatggtgatggtgtgctgctctcc-3'), cloned into pMal-linkerAAA (EcoRI/Sall)
pMal-linkerAAA-Nup214(1916-2033)-His	PCR Nup214 (5'-tttGAATTCtcaataaccttaacctatttggaa-3'/ 5'-tttGTCGACTtagtgatggtgatggtgatggtgtgctgctctcc-3'), cloned into pMal-linkerAAA (EcoRI/Sall)
pMal-linkerAAA-Nup214(1930-2021)-His	PCR Nup214 (5'-tttGAATTCtttgggtgattgccagctcgtcg-3'/ 5'-tttGTCGACTtatgcctgagcagctcagtg-3'), cloned into pMal-linkerAAA (EcoRI/Sall)
pGEX-Nup62	PCR Nup62 (5'-aaaGTCGACaaatgagcgggttaattttggag-3'/ 5'-aaaGCGGCCGCtcaaggtgatccgga-3'), cloned into pGEX-6P1 (NotI/Sall)
pGEX-RanBP3	cloned into pGEX-6P1 (BamHI/XhoI)

Supplemental Table Legends

Table S1: X-ray data collection, refinement and validation statistics for the Nup214 export complex; related to Figure 2.

Table S2 and S3: Intra- and Interprotein cross-links identified in the trimeric export complex with bound Nup214; related to Figure 3.

Protein-protein cross-links identified in the trimeric export complex with bound Nup214. The intra- (S1) and inter- (S2) cross-linked peptides with their respective cross-linked lysine residues are listed. The distances in Å according to the crystal structure are also listed. ND: not determined, as these parts are missing in the crystal structure. *, cross-links with distances >30 Å. These can be explained by the flexibility of the involved regions. For example, Lys1049 (crosslinking to Lys594^{CRM1}) is located in the C-terminal helix 21B of CRM1, which is known to adopt various orientations in different crystal structures. Lysine 221 of SPN1 (crosslinking to Lys159^{Ran}) is located in a loop region with increased flexibility, as reflected by its elevated B-factors. This is indicative of a high flexibility of the whole SPN1 loop 215-228 in the context of the export complex in solution.

Table S4: Plasmids generated in this study; related to Experimental Procedures.

Supplemental Experimental Procedures

Plasmids

Plasmids coding for CRM1 mutants were obtained by site-directed mutagenesis on the wild type plasmid.

A vector pMal-linkerAAA was cloned from the pMal-c2 vector with appropriate primers to resemble a previously published vector (Smyth et al., 2003).

Nup214-fragments were amplified by PCR and cloned into pMal-linkerAAA, pGEX-6P1 and pmRFP-cNLS (Roloff et al., 2013) *via* EcoRI/SalI.

Coding sequences for Nup214₁₈₅₉₋₂₀₉₀-X1/X2/X3 mutants were synthesized (GeneArt) and cloned into pmRFP-cNLS (Roloff et al., 2013) *via* EcoRI/SalI. Coding sequences for His-Nup214₁₉₁₆₋₂₀₃₃ and MBP-Nup214₁₉₁₆₋₂₀₃₃ mutants were amplified from the respective pmRFP-Nup214₁₈₅₉₋₂₀₉₀-cNLS plasmids and cloned into pET28a and pMal-linkerAAA *via* NdeI/XhoI and EcoRI/SalI, respectively.

The coding sequences of RanBP3 (isoform b) and Nup62 were amplified by PCR and cloned into pGEX-6P1 *via* BamHI/XhoI or NotI/SalI, respectively.

Further details about sequences and primers can be found in Table S3.

Protein Expression and Purification

Expression and purification of CRM1 (Dolker et al., 2013; Guan et al., 2000), importin β (Chi et al., 1997), importin 5 (Jäkel and Görlich, 1998), importin 13 (Mingot et al., 2001), transportin (Baake et al., 2001), RanGAP (Mahajan et al., 1997), Ran (Melchior et al., 1995), GST-SPN1 (Strasser et al., 2004), His-SPN1 (Waldmann et al., 2012), GST-Rev (Arnold et al., 2006), GST-Nup214 and His-Nup214₁₉₁₆₋₂₀₃₃ (Roloff et al., 2013) was adapted from published protocols.

CRM1 mutants were expressed in *E. coli* TG1 cells in 2YT medium supplemented with ampicillin. Cells were grown at 37 °C to an OD₆₀₀ of 0.7. Protein expression was induced by adding 0.1 mM IPTG and cells were grown at 37 °C for 5 hours. Cells were harvested (5000 xg, 20 minutes, 4 °C), washed with PBS and stored at -80 °C until purification. CRM1 mutants were purified as described for wild type CRM1.

H. sapiens His₁₀ZZ-[TEV]-RanGTP_{1-180, Q69L} (Monecke et al., 2009) was expressed in *E. coli* BL21(DE3)pLysS in 2YT medium supplemented with ampicillin, chloramphenicol and 2% (w/v) α-D-glucose to repress basal expression. Cells were grown at 37 °C to an optical density (OD₆₀₀) of 0.4 and temperature was gradually reduced to 18 °C in three steps. Protein expression was induced at an OD₆₀₀ of 0.9 adding IPTG to a final concentration of 0.5 mM. Cells were harvested after 15 h of induction (5000 xg, 20 minutes, 4 °C) and resuspended in lysis buffer (500 mM NaCl, 50 mM HEPES/NaOH pH 7.0, 5 mM MgCl₂, 3 mM imidazole, 10% (v/v) glycerol, 50 μM GTP and 1 mM DTT). Cells were disrupted using a Microfluidizer 110S (Microfluidics), and the clarified lysate (30,000 xg, 30 min, 4 °C) was applied onto a HisTrap column (GE Healthcare) equilibrated with lysis buffer. Unbound proteins were removed by washing with two column volumes of lysis buffer and bound His₁₀ZZ-RanGTP was eluted with lysis buffer containing 500 mM imidazole. For cleavage, the His₁₀-[TEV]-RanGTP fusion protein was incubated with TEV protease (Invitrogen) at 4 °C overnight in a 100:1 molar ratio. Pooled protein fractions were desalted in lysis buffer and loaded onto a second HisTrap column equilibrated with lysis buffer. The flow through containing RanGTP was collected, concentrated and passed over a Superdex S75 gel filtration column (GE Healthcare) equilibrated with 500 mM NaCl, 50 mM HEPES/NaOH pH 7.0, 5 mM MgCl₂, 10% (v/v) glycerol, 30 μM GTP and 1 mM DTT. RanGTP containing fractions were pooled, concentrated, frozen in liquid nitrogen and stored at -80 °C.

Expression and purification of *H. sapiens* SPN1₁₋₂₉₁ was analogous to full-length SPN1 (Strasser et al., 2004).

GST-Nup214 and His-Nup214 fragments were expressed and purified as described before (Roloff et al., 2013). Glutathione was removed from the eluted GST-Nup214 by buffer exchange into GST prep buffer (50 mM Tris pH 6.8, 300 mM NaCl, 1 mM MgCl₂, 0.25 mM EDTA, 1 mM DTT, 1 μg/ml each of leupeptin, pepstatin, and aprotinin) with PD-10 Desalting Columns (GE Healthcare). His-Nup214 fragments were additionally purified with a HiLoad 26/60 Superdex 75 prep grade column (GE Healthcare) in His prep buffer (50 mM Tris pH 6.8, 200 mM NaCl, 1 mM MgCl₂, 10% glycerol, 4 mM β-mercaptoethanol, 0.1 mM PMSF and 1 μg/ml each of leupeptin, pepstatin, and aprotinin). The fractions containing the His-Nup214 were determined via SDS-PAGE, pooled and concentrated with 20 ml/5 kDa MWCO Spin-XR concentrators (Corning).

Plasmids coding for _{MBP}Nup214_{His}-fragments contained a C-terminal His₆-tag and an N-terminal modified MBP-tag (Smyth et al., 2003). _{MBP}Nup214_{His}-fragments were expressed in *E. coli* BL21 (DE3) codon+ cells in MBP rich medium (1% trypton, 0.5% yeast extract, 0.5% NaCl and 0.2% glucose). Expression was induced with 300 μM IPTG and cells were grown overnight at 18 °C. _{MBP}Nup214_{His}-fragments were purified in His prep buffer (50 mM Tris pH 6.8, 200 mM NaCl, 1 mM MgCl₂, 10% glycerol, 4 mM β-mercaptoethanol, 0.1 mM PMSF and 1 μg/ml each of leupeptin, pepstatin, and aprotinin) with a two step protocol using binding to Ni-NTA sepharose followed by binding to amylose resin.

H. sapiens GST-RanBP3 was expressed in *E. coli* Rosetta II (DE3) cells in 2YT medium supplemented with ampicillin, chloramphenicol and 2% glucose. Cells were grown at 37 °C to an OD₆₀₀ of 0.8. Protein expression was induced by adding 0.5 mM IPTG and cells were grown overnight at 18 °C. Cells were harvested (5000 xg, 20 minutes, 4 °C), washed with PBS and stored at -80 °C until purification. Cells were resuspended in RanBP3 buffer (50 mM Tris pH 8.0, 250 mM NaCl, 2 mM MgCl₂, 2 mM EDTA, 2mM DTT 1 mM PMSF, 1 μg/ml of each leupeptin, pepstatin, and aprotinin) and lyzed using an EmulsiFlex-C3 (Avestin). The clarified lysate (100,000 xg, 30 min, 4 °C) was applied onto glutathion

sepharose (GE Healthcare) equilibrated with RanBP3 buffer at 4 °C for 1 hour. Unbound proteins were removed by three washing steps with RanBP3 buffer and one washing step with RanBP3 buffer supplemented with 1 M LiCl. Bound GST-RanBP3 was eluted with RanBP3 buffer containing 15 mM reduced glutathion. GST-RanBP3 was cleaved with PreScission protease (4 °C, overnight) and purified with a Superdex S200 gel filtration column (GE Healthcare) equilibrated in RanBP3 buffer. RanBP3 containing fractions were pooled, concentrated, frozen in liquid nitrogen and stored at –80 °C.

H. sapiens GST-Nup62 was expressed in *E. coli* BL21 codon+ cells in 2YT medium supplemented with ampicillin. Cells were grown at 37 °C to an OD₆₀₀ of 0.7. Protein expression was induced by adding 0.2 mM IPTG and cells were grown overnight at 18 °C. Cells were harvested (5000 xg, 20 minutes, 4 °C), washed with PBS and stored at -80 °C until purification. Cells were resuspended in Nup62 buffer (50 mM Tris pH 6.8, 300 mM NaCl, 1 mM MgCl₂, 5% glycerol, 1 mM DTT, 1 μg/ml each of leupeptin, pepstatin, and aprotinin) supplemented with 1.5% sarkosyl and lyzed using an EmulsiFlex-C3 (Avestin). The clarified lysate (100,000 x g, 30 min, 4 °C) was applied onto glutathion sepharose (GE Healthcare) equilibrated with Nup62 buffer at 4 °C for 1 hour. Unbound proteins were removed by three washing steps with Nup62 buffer and bound GST-Nup62 was eluted with Nup62 buffer containing 15 mM reduced glutathion. GST-Nup62 was either changed into Nup62 buffer without glutathion using PD-10 desalting columns (GE Healthcare) or cleaved with PreScission protease (4 °C, overnight). Cleaved Nup62 was purified with a Superdex S75 gel filtration column (GE Healthcare) equilibrated in Nup62 buffer. Nup62 containing fractions were pooled, concentrated, frozen in liquid nitrogen and stored at –80 °C.

Preparation, crystallization and structure determination of the Nup214 export complex

The CRM1-SPN1-RanGTP_{-MBP}Nup214 complex was assembled by mixing the individual components in a 1:3:5:5 molar ratio and subsequently purified using an Superdex 200 gel filtration column (GE Healthcare) in a buffer containing 50 mM NaCl, 20 mM Tris pH 7.5, 2 mM Mg(OAc)₂ and 2 mM DTT. The purified complex was concentrated to 5 mg/ml, frozen in liquid nitrogen and stored at -80 °C.

The CRM1-SPN1-RanGTP_{-MBP}Nup214₁₉₁₆₋₂₀₃₃ export complex was crystallized by mixing 2 μ l of a 5 mg/ml protein solution with 1 μ l of a condition containing 5% (w/v) polyethylene glycol (PEG) 8000, 0.2 M L-proline, 0.1 M Tris/HCl pH 7.5, 4 mM D-maltose and 180 mM LiCl. In order to control the number of crystals per well, several seeds were added to the condition after an incubation time of 20 minutes. Crystals belonging to the orthorhombic space group $C222_1$ grew at 20 °C after 5 days to a typical size of 150 x 150 x 80 μ m. After size optimization, crystals diffracted X-rays to a maximum resolution of 7 Å. The diffraction quality could be significantly improved by successive crystal dehydration. For that purpose, crystals were transferred stepwise to conditions with increasing PEG 8,000 concentrations (from 5% to 45% PEG 8,000 with 15 min of incubation between 5% steps). Notably, this treatment did not only improve the diffraction quality of the crystals but additionally resulted in a significant reduction of the unit cell lengths by \approx 10% (e.g. a axis from 126 Å to 112 Å (13%), b axis from 263 Å to 248 Å (6%) and c axis from 229 Å to 210 Å (8%). This corresponds to a remarkable decrease in crystal solvent content of 10% (from 69% to 59%). To further improve data quality and reduce scattering contribution from the surrounding liquid (e.g. background noise by the cryo condition) during data collection, the crystals were fished onto micro meshes (MiTeGen) and mounted on beamline 14.3 (BESSY II, Berlin) equipped with an HC1c crystal humidifier. After complete removal of the liquid surrounding the crystal using a paper wick, the crystals were flash cooled in liquid nitrogen and transferred to beamline 14.1 equipped with a 6M Pilatus detector. Complete datasets of two such treated

crystals were collected at beamline 14.1 (BESSY II, Berlin) (Mueller et al., 2012). Data were processed using XDS and XSCALE (Kabsch, 2010).

The structure was solved by means of molecular replacement with PHASER (McCoy et al., 2007) using the export complex CRM1-SPN1-RanGTP (PDBid 3gix) (Monecke et al., 2009) as a starting model. Subsequently, MBP (PDBid 1anf) (Quiocho et al., 1997) was fitted manually into positive $|F_o - F_c|$ difference density, since localization by molecular replacement routines of PHASER did not provide an unambiguous solution. The poor overall quality of the MBP density suggests that significant movement of MBP in the crystal lattice is possible, which is consistent with the overall elevated B-factors of the MBP residues. Hence, several parts of MBP, especially in its N-terminal lobe, are not defined in the electron density map. However, dissolved crystals analysed by SDS-PAGE clearly showed the presence of full-length MBP. Thus, in order to retain structural integrity of the crystal lattice and the MBP, the residues were not omitted. The final MBP model contains residues 7-112, 115-143, 150-167, 170-173, 176-183, 188-204, 210-224, 229-247 and 257-369.

After replacement and initial rigid body refinement, positive $|F_o - F_c|$ difference electron density near the MBP C-terminus and CRM1 H14-20 as well as at the CRM1 N-terminus (H2-4) allowed us to build three regions of Nup214, each containing a number of canonical FG-repeats. The structure was refined by iterative cycles of CNS (Brunger, 2007) and manual model building in Coot (Emsley et al., 2010). A series of mFo-DFc simulated annealing electron density omit maps as implemented in CNS were used to build the Nup214 sequence as well as ambiguous portions of the other proteins. A final round of refinement was done in Phenix (Adams et al., 2010). Figures were generated with PyMol (The PyMOL Molecular Graphics System, Version 1.5.0.4 Schrödinger, LLC.).

Identification of protein crosslinks by Mass Spectrometry

Tetrameric complexes containing CRM1, SPN1, RanQ69L₁₋₁₈₀GTP and a MBP-tagged-Nup214₁₉₁₆₋₂₀₃₃-fragment were assembled and purified by gel filtration in PBS. For crosslinking of 1300 pmol of the Nup214-complex (30 min at 25° C in a total volume of 1.5 mL), a BS3:protein ratio of 200:1 was used. In-solution digestion, reduction and alkylation of BS3 crosslinked complexes were performed as described (De et al., 2015) with minor modifications. Crosslinked complexes were reduced to 50 μ L, to which 50 μ L 8 M urea in buffer (100 mM phosphate, pH 7.5, 30 min, RT) was added. Reduction and alkylation were achieved by addition of 25 μ L 10 mM DTT (Calbiochem):Buffer (50:50, 30 min, RT) and 25 μ L of 60 mM IAA:Buffer (50:50, 30 min, RT). Modified trypsin (Promega) was added in a 1:20 w/w ratio for overnight hydrolysis. All reagents were purchased from Sigma-Aldrich, unless otherwise indicated.

The peptide mixture was desalted with C18 Sep Pak columns. Columns were conditioned with 0.4 mL MeOH (Lichrosolv, Merck), 0.5 mL 80% v/v ACN (Lichrosolv, Merck), 0.1% v/v TFA (Roth, Karlsruhe) and 0.5 mL 0.1% TFA. Digests were taken to 5% v/v ACN, 0.1% v/v TFA prior to loading. Column wash was performed with 2X 0.5 mL 0.1% v/v TFA, and elution of peptides was performed with 80% v/v ACN, 0.1% v/v TFA, 2X 0.4 mL. The eluate was dried in a rotary evaporator. Enrichment of crosslinked peptides by size exclusion chromatography (SEC) was performed as reported (Leitner et al., 2012). Peptides were reconstituted in 30% v/v ACN, 0.1% v/v TFA, injected onto a Superdex Peptide column and eluted at 50 μ L/min collecting fractions of 50 μ L. Fractions 9-18 were dried in a rotatory evaporator and reconstituted in 12 μ L LC-MS analysis buffer (5% ACN v/v, 0.1% v/v formic Acid, Fluka, Switzerland) and directly submitted to LC-MS analysis.

Protein-protein cross-linking samples were submitted to LC-MS/MS analysis immediately after their preparation. Protein-protein cross-linking samples were dissolved in 12 μ L sample solvent (5% v/v ACN, 1% v/v FA), of which 5 μ L were injected onto a Thermo Fisher

Scientific EASY-nLC coupled to a Q-Exactive mass spectrometer. Peptides were separated on a 12 cm, 75 μ M inner diameter C18 (120 Å, 5 μ m, Dr. Maisch) analytical column with an 81 min, 4-37% Buffer B gradient (95% ACN, 0.1%FA) and a flow rate of 320 μ L/min. Mass spectrometric analysis of protein-protein cross-linked peptides was performed with a TOP15 method in data dependent acquisition mode. MS1 ions were recorded in the range of 350-1600 m/z at 140000 resolution. Fragmentation was generated by HCD activation (collision induced dissociation, normalized collision energy=25), and only precursor ions of charge state 3-8 were selected for fragmentation. Fragment ions were acquired in the Orbitrap at 17500 resolution. Dynamic exclusion was set at 20 seconds.

Identification of crosslinks with pLink was performed as published previously (Yang et al., 2012), with the following parameters: carbamidomethylation of cysteine, fixed; methionine oxidation, variable, FDR=5%. Spectra were searched against a forward and reverse database containing the UNIPROT sequences of the protein complex components.

Multiple sequence alignment of CRM1 orthologs

The amino acid sequences of 16 CRM1 orthologs (*Homo sapiens*, *Saccharomyces cerevisiae*, *Trypanosoma cruzi*, *Schizosaccharomyces pombe*, *Rattus norvegicus*, *Mus musculus*, *Drosophila melanogaster*, *Candida albicans*, *Trypanosoma brucei*, *Dictyostelium discoideum*, *Xenopus laevis*, *Bos taurus*, *Aspergillus terreus*, *Pan troglodytes*, *Danio rerio* and *Chaetomium thermophilum*) were aligned with ClustalW2 (Larkin et al., 2007). The alignment was used in Chimera (Pettersen et al., 2004) to color CRM1 residues of the CRM1-SPN1-RanGTP_{-MBP}Nup214 complex according to their level of conservation.

Supplemental References

- Adams, P.D., Afonine, P.V., Bunkoczi, G., Chen, V.B., Davis, I.W., Echols, N., Headd, J.J., Hung, L.W., Kapral, G.J., Grosse-Kunstleve, R.W., et al. (2010). PHENIX: a comprehensive Python-based system for macromolecular structure solution. *Acta crystallographica. Section D, Biological crystallography* 66, 213-221.
- Arnold, M., Nath, A., Hauber, J., and Kehlenbach, R.H. (2006). Multiple importins function as nuclear transport receptors for the Rev protein of human immunodeficiency virus type 1. *J. Biol. Chem.* 281, 20883-20890.
- Baake, M., Doenecke, D., and Albig, W. (2001). Characterisation of nuclear localisation signals of the four human core histones. *J Cell Biochem* 81, 333-346.
- Brünger, A.T. (2007). Version 1.2 of the Crystallography and NMR system. *Nat Prot* 2, 2728-2733.
- Chi, N.C., Adam, E.J.H., and Adam, S.A. (1997). Different binding domains for Ran-GTP and Ran-GDP/RanBP1 on nuclear import factor p97. *J Biol Chem* 272, 6818-6822.
- De, I., Bessonov, S., Hofele, R., dos Santos, K., Will, C.L., Urlaub, H., Lührmann, R., and Pena, V. (2015). The RNA helicase Aquarius exhibits structural adaptations mediating its recruitment to spliceosomes. *Nat. Struct. Mol. Biol.* 22, 138-144.
- Dolker, N., Blanchet, C.E., Voss, B., Haselbach, D., Kappel, C., Monecke, T., Svergun, D.I., Stark, H., Ficner, R., Zachariae, U., et al. (2013). Structural Determinants and Mechanism of Mammalian CRM1 Allostery. *Structure* 21, 1350-1360.
- Emsley, P., Lohkamp, B., Scott, W.G., and Cowtan, K. (2010). Features and development of Coot. *Acta crystallographica. Section D, Biological crystallography* 66, 486-501.
- Guan, T., Kehlenbach, R.H., Schirmer, E.C., Kehlenbach, A., Fan, F., Clurman, B.E., Arnheim, N., and Gerace, L. (2000). Nup50, a nucleoplasmically oriented nucleoporin with a role in nuclear protein export. *Mol. Cell Biol.* 20, 5619-5630.

- Jäkel, S., and Görlich, D. (1998). Importin beta, transportin, RanBP5 and RanBP7 mediate nuclear import of ribosomal proteins in mammalian cells. *EMBO J.* 17, 4491-4502.
- Kabsch, W. (2010). Xds. *Acta crystallographica. Section D, Biol Crystal.* 66, 125-132.
- Larkin, M.A., Blackshields, G., Brown, N.P., Chenna, R., McGettigan, P.A., McWilliam, H., Valentin, F., Wallace, I.M., Wilm, A., Lopez, R., et al. (2007). Clustal W and Clustal X version 2.0. *Bioinformatics* 23, 2947-2948.
- Leitner, A., Reischl, R., Walzthoeni, T., Herzog, F., Bohn, S., Forster, F., and Aebersold, R. (2012). Expanding the chemical cross-linking toolbox by the use of multiple proteases and enrichment by size exclusion chromatography. *Mol Cell Proteomics* 11, M111014126.
- Mahajan, R., Delphin, C., Guan, T., Gerace, L., and Melchior, F. (1997). A small ubiquitin-related polypeptide involved in targeting RanGAP1 to nuclear pore complex protein RanBP2. *Cell* 88, 97-107.
- McCoy, A.J., Grosse-Kunstleve, R.W., Adams, P.D., Winn, M.D., Storoni, L.C., and Read, R.J. (2007). Phaser crystallographic software. *J Appl Crystall.* 40, 658-674.
- Melchior, F., Sweet, D.J., and Gerace, L. (1995). Analysis of Ran/TC4 function in nuclear protein import. *Methods Enzymol.* 257, 279-291.
- Mingot, J.M., Kostka, S., Kraft, R., Hartmann, E., and Görlich, D. (2001). Importin 13: a novel mediator of nuclear import and export. *Embo J.* 20, 3685-3694.
- Monecke, T., Güttler, T., Neumann, P., Dickmanns, A., Görlich, D., and Ficner, R. (2009). Crystal structure of the nuclear export receptor CRM1 in complex with Snurportin1 and RanGTP. *Science.* 324, 1087-1091. .
- Mueller, U., Darowski, N., Fuchs, M.R., Forster, R., Hellmig, M., Paithankar, K.S., Puhlinger, S., Steffien, M., Zocher, G., and Weiss, M.S. (2012). *J Synchr Rad.* 19, 442-449.

- Pettersen, E.F., Goddard, T.D., Huang, C.C., Couch, G.S., Greenblatt, D.M., Meng, E.C., and Ferrin, T.E. (2004). UCSF Chimera - a visualization system for exploratory research and analysis. *Journal of computational chemistry* 25, 1605-1612.
- Quioco, F.A., Spurlino, J.C., and Rodseth, L.E. (1997). Extensive features of tight oligosaccharide binding revealed in high-resolution structures of the maltodextrin transport/chemosensory receptor. *Structure* 5, 997-1015.
- Roloff, S., Spillner, C., and Kehlenbach, R.H. (2013). Several Phenylalanine-Glycine Motives in the Nucleoporin Nup214 Are Essential for Binding of the Nuclear Export Receptor CRM1. *J Biol Chem* 288, 3952-3963.
- Smyth, D.R., Mrozkiewicz, M.K., McGrath, W.J., Listwan, P., and Kobe, B. (2003). Crystal structures of fusion proteins with large-affinity tags. *Protein science : a publication of the Protein Society* 12, 1313-1322.
- Strasser, A., Dickmanns, A., Schmidt, U., Penka, E., Urlaub, H., Sekine, M., Lührmann, R., and Ficner, R. (2004). Purification, crystallization and preliminary crystallographic data of the m3G cap-binding domain of human snRNP import factor snurportin 1. *Acta Crystallogr D Biol Crystallogr.* 60, 1628-1631.
- Waldmann, I., Spillner, C., and Kehlenbach, R.H. (2012). The nucleoporin-like protein NLP1 (hCG1) promotes CRM1-dependent nuclear protein export. *J. Cell Science* 125, 144-154. .
- Yang, B., Wu, Y.J., Zhu, M., Fan, S.B., Lin, J., Zhang, K., Li, S., Chi, H., Li, Y.X., Chen, H.F., et al. (2012). Identification of cross-linked peptides from complex samples. *Nature methods* 9, 904-906.